Monthly Notices
of the
ROYAL ASTRONOMICAL SOCIETY

Mon. Not. R. Astron. Soc. **422,** 1178–1185 (2012) doi:10.1111/j.1365-2966.2012.20691.x

Quantitative photospheric spectral analysis of the Type IIP supernova 2007od

C. Inserra,[1,2,3★] E. Baron[3,4,5] and M. Turatto[6]

[1]*Dipartimento di Fisica ed Astronomia, Universita' di Catania, Sezione Astrofisica, Via S.Sofia 78, 95123 Catania, Italy*
[2]*INAF – Osservatorio Astrofisico di Catania, Via S.Sofia 78, 95123 Catania, Italy*
[3]*Homer L. Dodge Department of Physics and Astronomy, University of Oklahoma, Norman, OK 73019, USA*
[4]*Hamburger Sternwarte, Gojenbergsweg 112, 21029 Hamburg, Germany*
[5]*Computational Research Division, Lawrence Berkeley National Laboratory, MS 50F-1650, 1 Cyclotron Road, Berkeley, CA 94720, USA*
[6]*INAF – Osservatorio Astronomico di Trieste, Via Tiepolo 11, 34143 Trieste, Italy*

Accepted 2012 February 3. Received 2012 February 3; in original form 2011 May 23

ABSTRACT

We compare and analyse a time series of spectral observations obtained during the first 30 d of evolution of SN 2007od with the non-local thermodynamic equilibrium code PHOENIX. Despite some spectroscopic particularities in the Balmer features, this supernova appears to be a normal Type II, and the fits proposed are generally in good agreement with the observations. As a starting point, we have carried out an analysis with the parametrized synthetic spectrum code SYNOW to confirm line identifications and to highlight differences between the results of the two codes. The analysis computed using PHOENIX suggests the presence of a high-velocity feature in Hβ and an Hα profile reproduced with a density profile steeper than that of the other elements. We also show a detailed analysis of the ions velocities of the six synthetic spectra. The distance is estimated for each epoch with the spectral-fitting expanding atmosphere method. Consistent results are found using all the spectra which give the explosion date of JD 245 4403 (2007 October 29) and a distance modulus $\mu = 32.2 \pm 0.3$.

Key words: line: identification – supernovae: general – supernovae: individual: SN 2007od – galaxies: distances and redshifts.

1 INTRODUCTION

SN 2007od, was discovered on 2007 November 2.85 UT in the nearby galaxy UGC 12846 (Mikuz & Maticic 2007). Blondin & Calkins (2007) classified it as a normal Type IIP supernova (SN IIP) about two weeks after explosion, and reported some similarity with the spectrum of the SN II 1999em, 10 d after explosion. SN 2007od, exploded in the Magellanic Spiral (Sm:) galaxy UGC 12846, which has a heliocentric recession velocity of 1734 ± 3 km s^{-1}, a distance modulus of 32.05 ± 0.15 and an adopted reddening of $E_{\rm tot}(B-V) = 0.038$ (Inserra et al. 2011). Extensive studies of the photospheric and nebular periods have been presented in Andrews et al. (2010) and Inserra et al. (2011).

SN 2007od, showed a peak and plateau magnitude, $M_V = -18.0$ and -17.7, respectively (Inserra et al. 2011), brighter than common SNe IIP (Patat et al. 1994; Richardson et al. 2002), but the luminosity on the tail is comparable with that of the faint SN 2005cs (Pastorello et al. 2009). The luminosity on the tail was affected by the early formation of dust ($\lesssim$220 d after explosion; Andrews et al. 2010). Based on mid-infrared observations in the nebular phase, the amount of dust has been determined to be up to 4.2×10^{-4} M$_\odot$ (Andrews et al. 2010) and the ejected mass ^{56}Ni $\sim 2 \times 10^{-2}$ M$_\odot$ (Inserra et al. 2011).

This object also shows interaction with a circumstellar medium (CSM). There is some evidence, in the form of high-velocity (HV) features, for weak interaction soon after the outburst and solid observational evidence for interaction in the nebular phase (Inserra et al. 2011). However, due to the good temporal coverage, the position inside the host galaxy and the low observed reddening, this SN is a good candidate for analysis by the generalized stellar atmosphere code PHOENIX in order to learn more about its physical structure. In Section 2, we present the codes and the strategy applied for modelling. In Section 3, we show the synthetic spectra and the comparison with observed spectra, while in Section 4 we provide an analysis of the principal characteristics of the synthetic spectra. A conclusion follows in Section 5.

2 METHOD

The preliminary line identification in the spectra of SN 2007od, confirming those obtained by Inserra et al. (2011), has been performed using the fast, parametrized SN synthetic spectra code SYNOW. The

★E-mail: cosimo.inserra@oact.inaf.it

code is discussed in detail by Fisher (2000) and recent applications include Branch et al. (2002), Moskvitin et al. (2010) and Roy et al. (2011). SYNOW assumes the Schuster–Schwarzschild approximation and the source function is assumed to be given by resonant scattering, treated in the Sobolev approximation. It correctly accounts for the effects of multiple scattering.

For a subsequent, more detailed analysis, we have used the generalized stellar atmospheres code PHOENIX (Hauschildt & Baron 2004, 1999). The code includes a large number of non-local thermodynamic equilibrium (NLTE) and LTE background spectral lines and solves the radiative transfer equation with a full characteristics piecewise parabolic method (Hauschildt 1992) without simple approximations such as the Sobolev approximation (Mihalas 1970). The process that solves the radiative transfer and the rate equations with the condition of radiative equilibrium is repeated until the radiation field and the matter converge to radiative equilibrium in the Lagrangian frame. These calculations assume a compositionally homogeneous atmosphere with a power-law density and steady-state conditions in the atmosphere.

3 SPECTRA MODELS

We have modelled the first six observed photospheric spectra, covering a period from 5 to 27 d since the adopted explosion date JD = 245 4404 ± 5 (∼2007 October 30; Inserra et al. 2011). The most interesting spectra are the first one of the series (5 d), with a flat-top Hα profile and two uncommon features at about 4400 and 6250 Å, and the last one (27 d), which has the best signal-to-noise ratio (S/N) among the plateau spectra. The detailed, comparative study of these epochs provides important information about the presence of ions and possible CSM interaction at early times.

Fig. 1 shows the line identifications determined by the SYNOW analysis for the first spectrum, obtained using $T_{\rm bb} \sim 12\,000$ K, $v_{\rm phot} \sim 7800\,{\rm km\,s^{-1}}$, optical depth $\tau(v)$ parametrized as a power law of index $n = 9$ and $T_{\rm exc} = 10\,000$ K assumed to be the same for all ions. The features visible in Fig. 1 are produced by only six chemical species. The P Cygni profiles of the Balmer lines are clearly visible, as well as He I λ5876, and significant contributions due to Ca II, Fe II, Ba II and Si II. The Balmer lines have been detached from the photosphere to better match the observed velocity. The uncommon lines mentioned above are identified as Ba II (λ4524) and Si II (λ6355). In our attempts, we have considered also the possible presence of N II λ4623, but the poor fit and the lack of N II λ5029 and N II λ5679 lines (stronger than the first one) lead us to the conclusion that there is no enhanced N in the spectra of SN 2007od, (cf. Inserra et al. 2011).

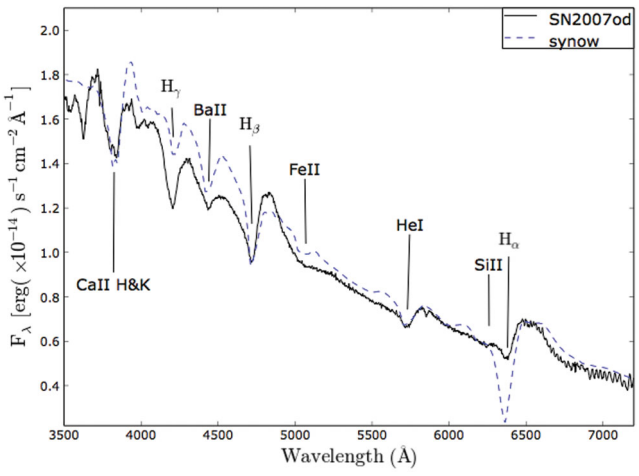

Figure 1. Comparison between the optical spectrum of SN 2007od, at 5 d post-explosion (JD 245 4404) and the SYNOW synthetic spectrum (for composition of synthetic spectra, see text).

Table 1. Parameters of PHOENIX models of SN 2007od,.

JD +240 0000	Phase[a] (d)	$T^{b}_{\rm model}$ (K)	v_0 (km s^{-1})	n^{c}	r (10^{14} cm)	L (10^{41} erg s^{-1})
54409.5	5.5	8000	7600	13	3.6	3.8
54412.5	8.5	7400	7200	9	5.3	6.0
54413.2	9.2	7300	7050	9	5.6	6.3
54417.4	13.4	6800	6000	9	6.9	7.2
54421.4	17.4	6200	5400	9	8.1	6.9
54431.5	27.5	6000	5000	9	11.9	13.1

[a]With respect to the explosion epoch (JD 245 4404) from Inserra et al. (2011).
[b]With a total $E(B-V) = 0.038$ (Inserra et al. 2011).
[c]Index of power-law density function.

With the adopted reddening [$E(B-V) = 0.038$] and the ions suggested by the SYNOW analysis, we have computed a grid of detailed fully line-blanketed PHOENIX models. We have explored variations in multiple parameters for each epoch adjusting the total bolometric luminosity in the observer's frame (parametrized by a model temperature, $T_{\rm model}$), the photospheric velocity (v_0), the metallicity (the solar abundances were those of Grevesse & Sauval 1998) and the density profile (described by a power law $\rho \propto r^{-n}$). Gamma-ray deposition was assumed to follow the density profile. We noted an increase of the emission profiles, especially those of Balmer lines, with the increase of gamma-ray deposition. However, in our final models the gamma-ray deposition was not included. We have estimated the best set of model parameters by performing a simultaneous χ^2 fit of the main observables. The relevant parameters for SN 2007od, for the entire early evolution are reported in Table 1, while the fits are shown in Figs 2 and 3.

In the first PHOENIX spectra, we have treated in NLTE the following ions: H I, He I, He II, Si I, Si II, Ca II, Fe I, Fe II, Ba I, Ba II. He I, Si I, Fe I and Ba I have been considered to reproduce the ionization levels of the corresponding atoms. The opacity for all other ions is treated

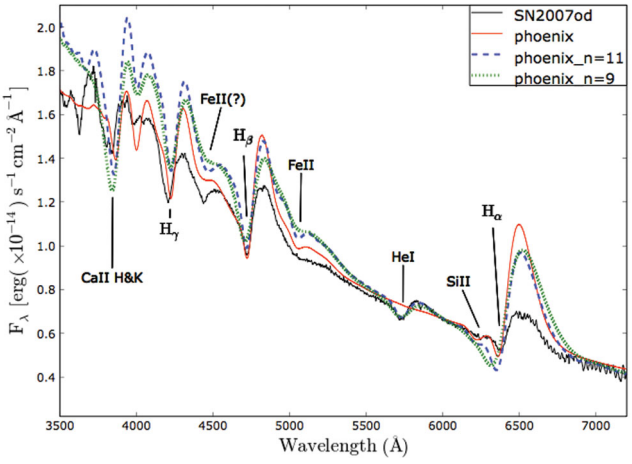

Figure 2. Comparison between the optical spectrum of SN 2007od, at 5 d post-explosion (JD 245 4404) and PHOENIX full NLTE spectra. The model parameters are those of the first row of Table 1 but for the n index reported in the legend.

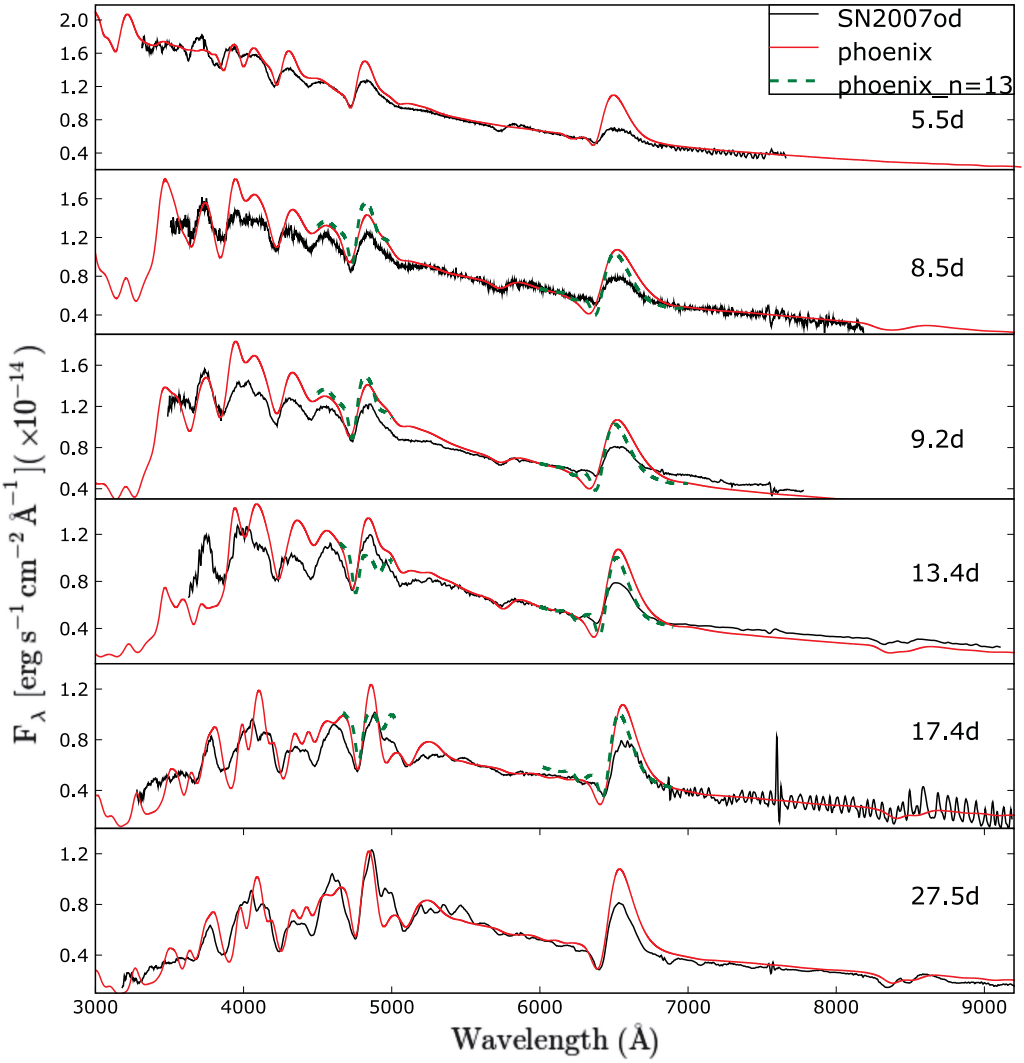

Figure 3. PHOENIX spectral evolution compared with observed spectrum. Model parameters for best-fitting spectra (red) are listed in Table 1. The dashed green lines in the spectra between day 8.5 and 17.4 in the Hβ and Hα regions are the line profiles computed with a density index $n = 13$.

in LTE with a constant thermalization parameter $\epsilon = 0.05$ (see Baron et al. 1996b, for further details). As shown in Fig. 2, there is no line that corresponds to Ba II, even though the identification for the absorption at 4400 Å seemed plausible in the SYNOW analysis. The temperature is too high to produce a Ba II line, all the more so with the observed strength. The presence of Ba II was checked by calculating a set of single ion spectra, i.e. calculating the spectrum with all continuum opacities, and only lines from Ba II as well as via the inverse procedure of turning off the line opacity from Ba II. The same procedure was performed for the He I ion, in order to study the feature that could arise around 4471 Å but no significant contribution can be seen in the synthetic spectra. The closest line to the 4440 Å feature is due to Fe II, though it is not as strong as in the observed spectrum. The evolution of the 4440 Å region (shown in Fig. 4) displays the inconsistency. The Fe II line explains the feature starting from day 9, though the velocity does not match the observed line position. It is likely that the observed profile of the 4440 Å feature is due to the combination of this line with HV feature of Hβ, formed by an increased line opacity that our simplified model ($\rho \propto r^{-n}$) is not able to reproduce (the HV features are discussed in Inserra et al. 2011). Though Ba II identification provided by SYNOW is not completely ruled out by the NLTE analysis, however, we consider it unlikely.

The presence of Si II at 6530 Å is confirmed by the PHOENIX analysis, despite the weakness of the synthetic feature. In Fig. 2, it is barely visible, but the same analysis performed for Ba II confirms its identification. The presence of Si II in SNe IIP is not uncommon. The other absorption features are successfully reproduced, except for Hα (see Section 4) and the absorption lines in the region of 3600 Å that are possibly related to Ti II, not included in the first NLTE spectra in order to minimize CPU time. As shown in Fig. 2, we tried different density indices to better match the entire profile. The best match for the overall spectrum is given by the model with $n = 13$ (in all figures, the best PHOENIX model is always plotted in red), even if the strengths, with respect to the normalized continuum, of Hγ and He I are better reproduced by the models with a density exponent lower than $n = 13$. The steeper density profile leads to greater emission than models with flatter density profiles.

Both the second (8.5 d) and third (9.2 d) spectra have been constructed using the same set-up that was used to calculate the first spectrum, except that the density index was decreased from 13 to 9. A profile steeper than $n = 9$ better reproduces the absorption profile

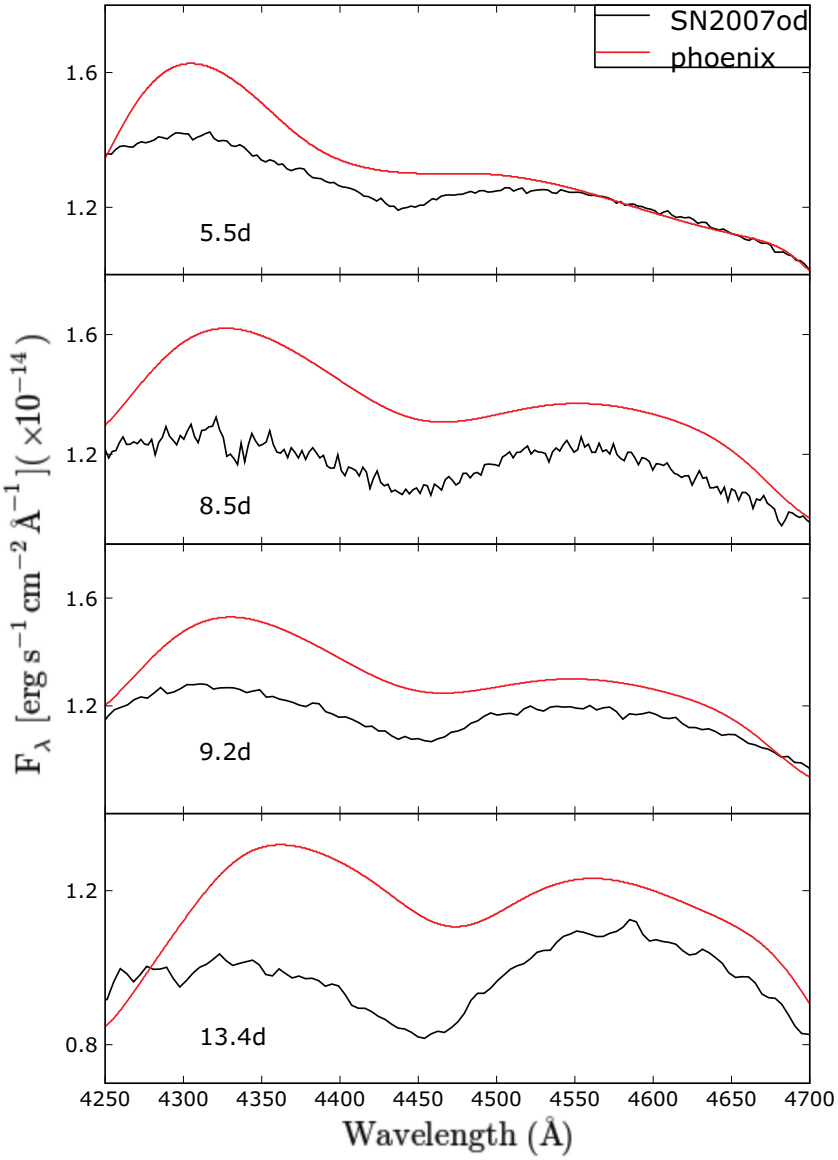

Figure 4. A blow-up of the 4440 Å region where the PHOENIX synthetic spectra are compared to observed ones.

of the Balmer lines, as seen in first epoch, but all the models show flux slightly higher bluewards of 5500 Å and especially at about 4000 Å. Also the strength of Hγ is greater than observed in the model with $n > 9$. The flux on the blue side of Ca II H&K is lower than observed. We found that a steeper density profile enhances the discrepancy between the observed and synthetic H&K line profile.

In general, the line profiles suggest a density distribution more complex that a single power law. Our calculations suggest that perhaps a broken power law would better reproduce the observed spectra, with a shallower density profile at lower velocities and a steeper profile at higher velocities. The Ca II or He I ions are clearly better reproduced by a density index close to 9, while the metal elements (e.g. Fe and Si) which form close to the photosphere (and are relatively weak) are less sensitive to the assumed density profile. The Fe I, Fe II and Si II are well reproduced with all density profiles, even if the steeper profile better reproduces the Si II profile than the flatter profile (see Fig. 2). While the more complex density profile could be intrinsic in the initial structure, it is also possible that early interaction of the SN ejecta with a close-in circumstellar region affects the line profiles. Indeed, the flat-topped nature of the Balmer lines may indicate circumstellar interaction. A broken power-law density distribution of the ejecta has been claimed also by Utrobin & Chugai (2011) in the case of SN 2000cb. To illustrate the case, we have overplotted in Fig. 3 the Hβ and Hα regions obtained by $n = 13$ models (green dashed line) for the spectra from 8.5 to 17.4 d.

The spectra at 13.4 and 17.4 d show the increasing effects of a few metal lines such as Fe II λ5169 and Sc II λ6300 that indicate the lower temperature at the beginning of the plateau phase. Moreover, the presence of metal ions changes the flux at ∼3800 Å in the spectra at 13 d. From this epoch onwards, the 4440 Å feature seems more clearly related to Fe II, strengthening our conclusion for the absence of Ba II.

The final spectrum we analyse was obtained on 2007 November 27 (27 d) when the SN is solidly on the plateau. At this epoch, the metal lines are fully developed, as is the Na I D feature that has replaced the He I λ5876 line. Thanks to the broad wavelength coverage, the good resolution (11 Å) and the high S/N (60), this is the best available spectrum of SN 2007od.

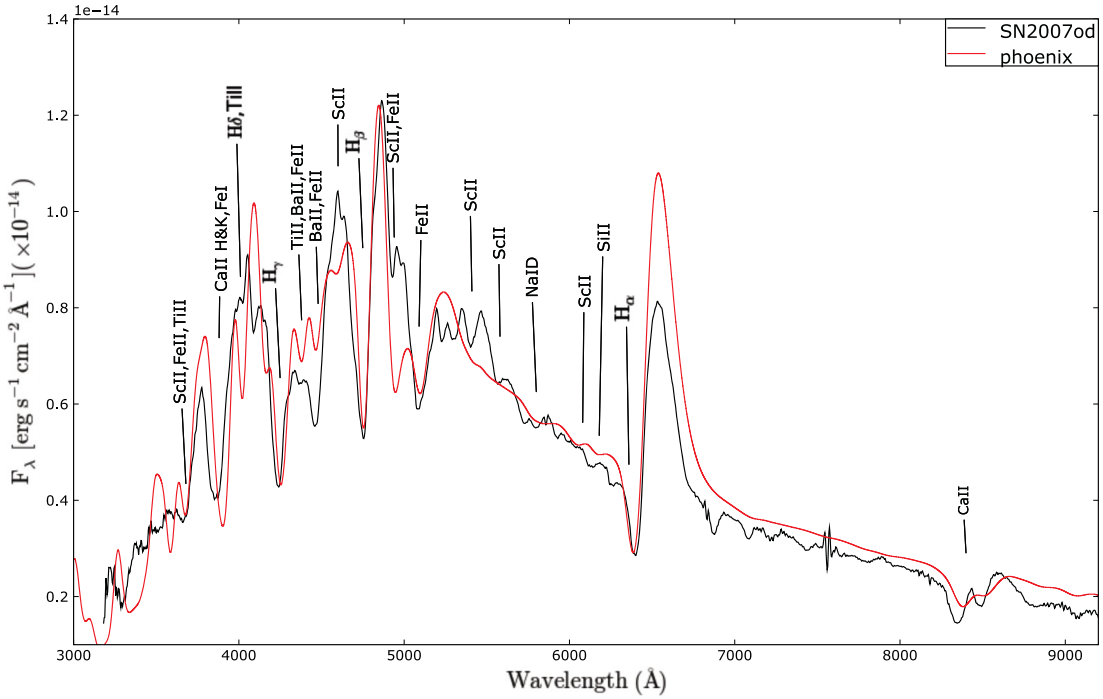

Figure 5. Comparison between the optical spectrum of SN 2007od, at 27 d post-explosion (JD 245 4404) and the PHOENIX full NLTE spectrum (for model parameters, see Table 1).

Fig. 5 displays our best NLTE model. The species treated in NLTE are H I, Na I, Si I, Si II, Ca II, Sc I, Sc II, Ti I, Ti II, Fe I, Fe II, Ba I and Ba II. Here, more than at earlier epochs, the presence of the neutral species changes the strength of some lines, especially in the blue (<4000 Å) and around 5000 Å. The H lines, Na I D, Fe II λ5169, Sc II λ5658 and Sc II λ6245 are well fitted. The Ca II lines also are well fitted. Other lines fit fairly well in terms of velocity width, but not necessarily in total flux. This is due to the fact that many lines are blended with others.

All models have solar abundances and metallicity. We studied the effects of reducing the model metallicity to that deduced for the SN 2007od, environment ($Z < 0.004$; see Inserra et al. 2011), but the changes in the spectra were negligible at the 3σ level.

The comparative evolution of SN 2007od has been discussed in section 3.3 of Inserra et al. (2011). The most interesting features noted in the earliest phases were the 4400 Å absorption and the boxy profile of the Balmer lines. In Fig. 6, we compare the spectra of SN 2007od at two phases (day 5.5 and day 27) with those of SN 1999em, the most similar SN IIP as determined by GELATO analysis (Harutyunyan et al. 2008), and with the two corresponding best synthetic spectra. Indeed, the overall similarity is remarkable. However, there are also interesting differences, in addition to the two major ones mentioned above. At the first epoch, the expansion velocity is larger in SN 1999em [full width at half-maximum, $\mathrm{FWHM}(\mathrm{H}\alpha)_{99\mathrm{em}} \sim 11000 > \mathrm{FWHM}(\mathrm{H}\alpha)_{07\mathrm{od}} \sim 9000\,\mathrm{km\,s^{-1}}$], while at the second epoch SN 2007od is faster than SN 1999em [$\mathrm{FWHM}(\mathrm{H}\alpha)_{07\mathrm{od}} \sim 7000 > \mathrm{FWHM}(\mathrm{H}\alpha)_{99\mathrm{em}} \sim 5500\,\mathrm{km\,s^{-1}}$]. However, the epochs are offset, so evolution could play a role. The slower velocity evolution of SN 2007od was already noted by Inserra et al. (2011). The model is able to reproduce consistently the spectra of SN 2007od at both epochs. The other major difference is in the line contrast. Considering the ongoing early interaction, we can interpret the effect as due to toplighting (Branch et al. 2000), which smooths the line contrast. At the second epoch, the difference between the line profiles of the two objects and the model is reduced.

4 ANALYSIS

The expansion velocities of Hα, Hβ, He I λ5876 and Fe II λ5169 as derived from fitting the absorption minima of the PHOENIX spectra are shown in Fig. 7, together with the measured values in the observed spectra. The filled symbols indicate the spectra shown in Fig. 3 (reported in Table 1), while the open symbols refer to spectra calculated with different density indexes ($n = 9$ for the first epoch, $n = 13$ for the following epochs).

In Figs 7 (top left-hand panel) and 3, the absorption minima in the NLTE ($n = 9$) spectra for Hα are too blue when compared with the observed spectra, particularly for the first three epochs. Instead, the models with $n = 13$ better reproduce the observed velocity. This could be due to several effects. The simple uniform power-law density profile, assumed here, may not be accurate enough to describe the ejecta. Also, ionization effects, perhaps due to circumstellar interaction, may reduce the Balmer occupations over those that are predicted in the $n = 9$ models. Combined with the evidence of the flat-top emission, it is somewhat possible that circumstellar interaction effects are responsible for the observed shape of the Balmer lines and for the different density profiles. The effect disappears with time. Also for Hβ, the PHOENIX and the observed velocity from 13.4 d are comparable within the errors for both models. From day 8.5 and onwards, the $n = 9$ models better reproduce the Hβ profile in velocity and strength. Neither He I nor Fe II shows this behaviour in the early epochs, indicating that the effect is most likely confined to the outermost layers of the ejecta. Except for the epochs reported above, all the line velocities are slightly smaller than observed. Though we have not included time-dependent rates in this calculation, this effect seems not so likely to explain the discrepancy

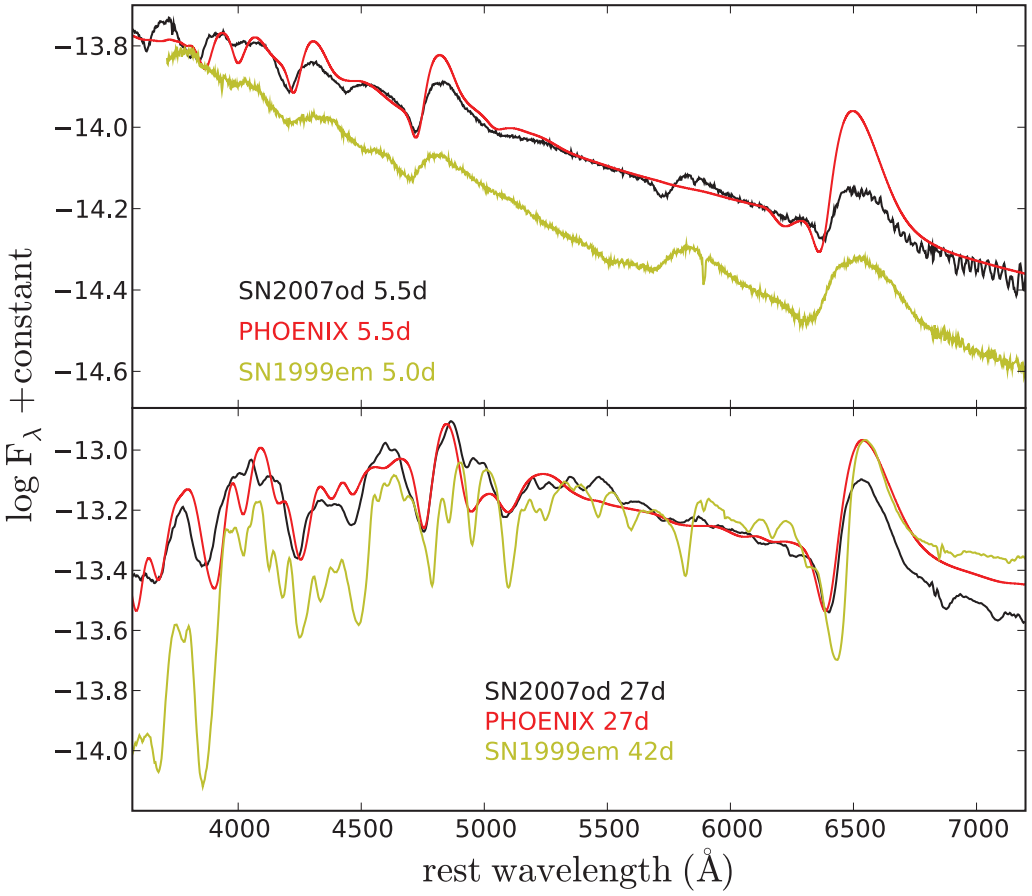

Figure 6. Comparison between observed spectra of SN 2007od, PHOENIX full NLTE spectra (for model parameters, see Table 1) and SN 1999em spectra at the first (top) and last epoch (bottom) of our series.

between the velocity of the synthetic and observed Hα (Utrobin & Chugai 2005; Dessart & Hillier 2007; De, Baron & Hauschildt 2009, 2010).

Clearly, our simplistic models do not reproduce the HV feature of Hβ and overestimate the emission strength of Hα, especially in the first spectrum. While interaction of the SN ejecta with circumstellar matter may be important, it is also possible that the density distribution we have adopted is too simplistic. The latter highlights the need for using the correct physical structure when modelling the SNe.

The sample of photospheric NLTE spectra collected for the SN 2007od, allow us to apply the spectral-fitting expanding atmosphere method (SEAM; Baron et al. 1993, 1995, 1996a; Baron, Hauschildt & Branch 1994) since, in addition to a good overall shape of the spectra, the models predict consistent fluxes. We can derive a distance modulus by subtracting our calculated absolute magnitudes from the published photometry (Inserra et al. 2011), assuming a reddening of $E(B-V)_{\rm tot} = 0.038$. Considering all the epochs, we obtain the distance modulus of the SN, $\mu = 32.5 \pm 0.3$, where the errors include the standard deviation of our fits and the error due to the uncertainty in the interstellar reddening. Since SEAM is strongly dependent on the uncertainties of the explosion date, it seems reasonable to give lower weight to early spectra, since a longer time baseline minimizes the error due to the uncertainties in the explosion day. If we consider only the later observed spectra, from 13.4 to 27.5 d, we find $\mu = 32.2 \pm 0.2$, in good agreement with the value reported in Inserra et al. (2011). Furthermore, model spectra for the last three epochs better fit the observations over the entire spectral range, and the derived distance modulus is comparable with the Mould et al. (2000) measurement within the uncertainties.

Indeed, a good agreement with the Inserra et al. (2011) distance ($\mu = 32.2 \pm 0.3$) is obtained by using all spectra and by taking the explosion date to be JD 245 4403 (2007 October 29). Hence, we conclude that the explosion date is October 29 $\pm$ 1.5 d. The explosion date should always be determined by a χ^2 minimization in a SEAM analysis.

5 CONCLUSIONS

We have shown that both direct synthetic spectral fits and detailed NLTE models do a good job in reproducing the observed optical spectra of SN 2007od,. We have also pointed out that detailed NLTE spectral modelling of early spectra does not support the line identification (Ba II, Fe II or He I) of the 4440 Å as suggested by the SYNOW model or as identified in previous SNe IIP. Rather, we interpret the line as a combination of Fe II and with an additional contribution from a possible HV feature of Hβ. The origin of the line could be due to increased opacity at high velocities due to variation in the level populations not accounted in the simple density profile of PHOENIX or due to possible interaction in the outermost layers. This result suggests extreme caution with line identifications in hot, differentially expanding flows. At the same time, it shows that PHOENIX calculations give reliable results and lend support to the reliability of the modelling. Our spectral analysis shows that during the plateau Sc II lines can arise even with standard solar abundances.

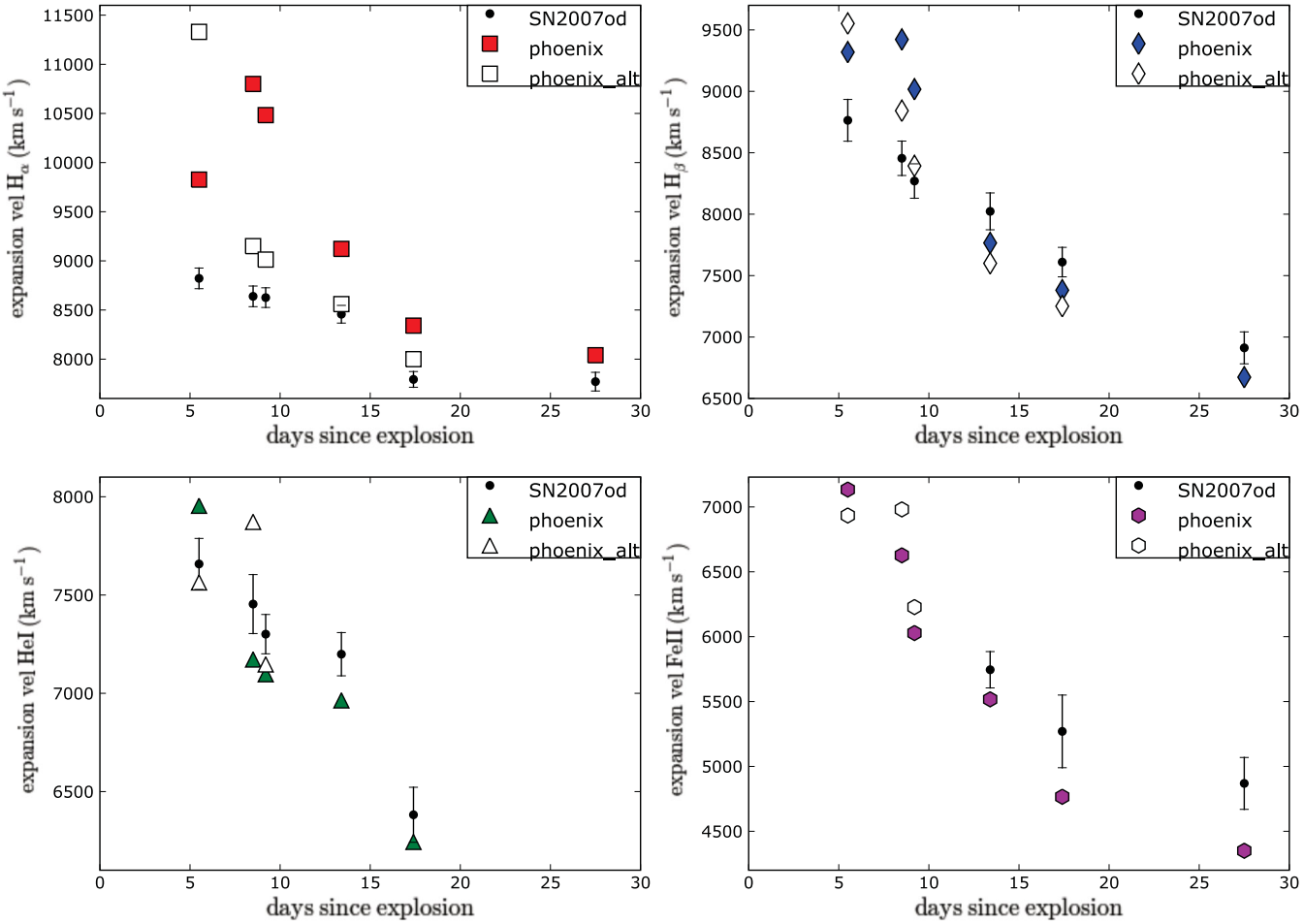

Figure 7. Expansion velocities of Hα, Hβ, He I and Fe II measured from synthetic PHOENIX NLTE spectra compared with those measured from the observed spectra (black dots with error bars) by Inserra et al. (2011). Filled symbols refer to the spectra shown in Fig. 3, while open symbols to spectra calculated with different density indexes ($n = 9$ for the first epoch, $n = 13$ for the following).

Also Si II lines are reliably identified in the spectra of our relatively normal SN IIP at early times. Another important issue is related to the difference between the density profile ($\rho \propto r^{-13}$) needed to reproduce Hα from 8.5 to 17.4 d and the density law required to reproduce the other elements ($\rho \propto r^{-9}$). The evidence for a broken power-law density profile shown by SN 2007od could be a general property of SNe II or may be a consequence of a perturbed ejecta, especially in the outermost layers. We have also discussed the velocity and strength evolution of the principal lines. We have also applied the SEAM to SN 2007od, obtaining good agreement with the distance modulus provided in Inserra et al. (2011) which allows us to better constrain the explosion date (2007 October 29).

ACKNOWLEDGMENTS

This work was supported in part by NSF grant AST-0707704, and US DOE Grant DE-FG02-07ER41517 and NASA programme number HST-GO-12298.05-A. Support for programme number HST-GO-12298.05-A was provided by NASA through a grant from the Space Telescope Science Institute, which is operated by the Association of Universities for Research in Astronomy, Incorporated, under NASA contract NAS5-26555. CI thanks David Branch for the useful discussions. MT is partially supported by the PRIN-INAF 2009 Supernovae Variety and Nucleosynthesis Yields'. We thank the anonymous referee for the useful suggestions that improved our paper.

REFERENCES

Andrews J. E. et al., 2010, ApJ, 715, 541
Baron E., Hauschildt P. H., Branch D., Wagner R. M., Austin S. J., Filippenko A. V., Matheson T., 1993, ApJ, 416, L21
Baron E., Hauschildt P. H., Branch D., 1994, ApJ, 426, 334
Baron E. et al., 1995, ApJ, 441, 170
Baron E., Hauschildt P. H., Branch D., Kirshner R. P., Filippenko A. V., 1996a, MNRAS, 279, 799
Baron E., Hauschildt P. H., Nugent P., Branch D., 1996b, MNRAS, 283, 297
Blondin S., Calkins M., 2007, Cent. Bureau Electron. Telegrams, 1119, 1
Branch D., Jeffery D. J., Blaylock M., Hatano K., 2000, PASP, 112, 217
Branch D. et al., 2002, ApJ, 566, 1005
De S., Baron E., Hauschildt P. H., 2009, MNRAS, 401, 2081
De S., Baron E., Hauschildt P. H., 2010, MNRAS, 407, 658
Dessart L., Hillier D. J., 2007, MNRAS, 383, 57
Fisher A., 2000, PhD thesis, Univ. Oklahoma
Grevesse N., Sauval A. J., 1998, Space Sci. Rev., 85, 161
Harutyunyan A. H. et al., 2008, A&A, 488, 383
Hauschildt P. H., 1992, J. Quant. Spectrosc. Radiative Transfer, 47, 433
Hauschildt P. H., Baron E., 1999, J. Comput. Applied Math., 109, 41
Hauschildt P. H., Baron E., 2004, Mitt. Math. Ges., 24, 1
Inserra C. et al., 2011, MNRAS, 417, 261

Mihalas D., 1970, Stellar Atmospheres. Series of Books in Astronomy and Astrophysics. Freeman, San Francisco
Mikuz H., Maticic S., 2007, Cent. Bureau Electron. Telegrams, 1116, 1
Moskvitin A. S., Sonbas E., Sokolov V. V., Fatkhullin T. A., Castro-Tirado A. J., 2010, Astrophys. Bull., 65, 132
Mould J. R. et al., 2000, ApJ, 529, 786
Pastorello A. et al., 2009, MNRAS, 394, 2266
Patat F., Barbon R., Cappellaro E., Turatto M., 1994, A&A, 282, 731
Richardson D., Branch D., Casebeer D., Millard J., Thomas R. C., Baron E., 2002, AJ, 123, 745
Roy R. et al., 2011, MNRAS, 414, 167
Utrobin V., Chugai N., 2005, A&A, 441, 271
Utrobin V. P., Chugai N. N., 2011, A&A, 532, A100

This paper has been typeset from a TEX/LATEX file prepared by the author.